Local entropy in quasi-one-dimensional heat transport

Chang Sub Kim[1,2,*] and Gary P. Morriss[2,†]
[1]*Department of Physics, Chonnam National University, Gwangju 500-757, Republic of Korea*
[2]*School of Physics, University of New South Wales, Sydney, New South Wales 2052, Australia*
(Received 9 August 2009; published 29 December 2009)

We study the nonequilibrium entropy of the heat transport problem by performing molecular dynamics simulations of a quasi-one-dimensional gas of hard disks in the steady state. The entropy density, flux, and production rate, associated with the entropy balance of the system, are obtained from the numerically measured velocity distributions, based on the kinetic theory analysis of the Boltzmann entropy. We obtain an equilibriumlike Clausius relation from the computer experiments which, in turn, fulfills the generalized Gibbs relation for spatially inhomogeneous states.

DOI: 10.1103/PhysRevE.80.061137 PACS number(s): 05.20.Dd, 05.70.Ln, 51.30.+i

I. INTRODUCTION

The notion of entropy lies at the heart of nonequilibrium (NE), or irreversible thermodynamics, however, to date no appropriate theoretical definition has been given for NE entropy itself. A plausible, immediate attempt is to replace the equilibrium ensemble density by the time-dependent precursor to the Gibbs equilibrium entropy. Unfortunately, this generalization fails to provide a proper representation of the NE entropy because it turns out to be a constant of motion for a closed system governed by Hamiltonian dynamics [1]. Thus, it does not accommodate the second law of thermodynamics as the spontaneous increase in entropy in the course of time for an isolated system prepared initially in a NE condition. Under this awkward situation, one is still required to furnish a balance equation for some entropy in order to facilitate the phenomenology of irreversible thermodynamics [2].

An exceptional case is found for a low-density gas and for that Ludwig Boltzmann provided us with the H theorem [3]. Accordingly, when the negative of the H function is accepted as a NE entropy for a dilute system, the statement of the second law of thermodynamics makes perfect sense. The probability density entering into the Boltzmann entropy is the one-particle reduced distribution function which is to be determined from the Boltzmann kinetic equation. Thus, kinetic theory provides a perceptible definition of the NE entropy for dilute systems at the cost of giving up the exact, N particle dynamics but sampling it by an effective one-particle dynamics.

In this work we adopt the Boltzmann entropy as a NE entropy to investigate NE thermodynamics. The system considered is a quasi-one-dimensional (QOD) low-density gas of hard disks with each end in contact with a heat reservoir at different temperatures. The hard disks collide with the walls according to the microscopic model of boundary scattering. The QOD system is chaotic, so as a consequence, it shows local thermal equilibration between the two (x and y) components of the kinetic energy achieved through particle dynamics alone. The extra advantage of the QOD model is that particles are ordered in space. Accordingly, the local properties are related to a single particle, which allows a very convenient access to the study of local properties. In the steady state temperature gradients set up, which play the role of a thermodynamic force to generate a heat flux along the structure. We perform molecular-dynamics (MD) simulations under this NE condition to obtain the velocity distributions of each particle and utilize them to calculate the nonequilibrium properties associated with the entropy balance of the system.

The major goal of this work is to study the *local properties* of the NE entropy of the system in the steady state *directly* from MD computer experiments and compare the results with those of the Boltzmann equation. Our NEMD method is not restricted to small temperature gradients; however we limit our attention mainly to the small gradient regime where one finds that the conventional description of linear irreversible thermodynamics applies. It is of central importance to construct an appropriate, first law of thermodynamics in local form, namely a generalized Gibbs relation, in irreversible thermodynamics. The first law of thermodynamics is a general statement about the energy balance in the system of interest, which is typically open to the surrounding [4]. Accordingly, it holds not only for reversible but also NE irreversible changes of the system. The utility of the first law is to provide a means to calculate the various thermodynamic properties, thus to provide, in particular, a meaning for the thermometric as well as calorimetric measures in real experiments.

There are other studies of the NE entropy; however, it is rare to find such investigations in the literature where the local properties of the NE entropy are investigated. This may have something to do with the fact that a quantitative investigation of spatially inhomogeneous NE states is quite a demanding task. Most systems investigated previously were assumed to be homogeneous in that the locality of the entropy density did not enter into the problem. Instead, the NE state was characterized by an external parameter like shear rate in the uniform shear flow problems [5–7]. Then, the uniform entropy as a function of the shear rate was of major interest analytically, not restricted to a small shear rate in the low-density regime where the Boltzmann entropy prevails. In addition, there appear earlier considerations of NE entropies for dense systems. The revised Enskog equations were employed to study the formal aspect of establishing irreversibility of

*cskim@jnu.ac.kr
†g.morriss@nsw.edu.au

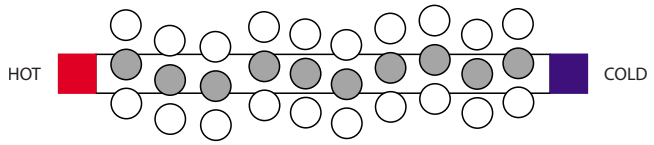

FIG. 1. (Color online) Schematic of the QOD system of hard disks which extends along x, where the longitudinal length and transverse width are L_x and L_y, respectively, and the radius of the hard disk is assumed to be a.

dense gases, similar to Boltzmann's H theorem, however no connection was made with a concrete physical system [8,9]. Also, by utilizing the Green expansion of the generalized Gibbs entropy, the steady-state entropy of a moderate dilute liquid of soft disks was investigated by computer simulation with the Gaussian thermostat [10]. Further, a direct NEMD calculation of the entropy change of the steady state of the same shear flow was applied in order to bypass the complexity of handling Green's expansion numerically [11]. However, again the fluid was assumed to be homogeneous and for both cases the NE entropies studied were all uniform in space unlike our investigation.

This paper is organized as followings. In Sec. II we describe our QOD heat transport model with a brief account of NEMD method used. In Sec. III the kinetic theory basis of the entropy balance equation is given with the Boltzmann entropy. In the subsequent Sec. IV the various NE thermodynamic properties associated with the nonuniform entropy density are presented. Finally, a summary is followed in Sec. V.

II. QUASI-ONE-DIMENSIONAL HEAT TRANSPORT MODEL: NEMD

We depict the QOD system of N-identical hard disks schematically in Fig. 1. The system is in contact with a hot reservoir with temperature T_L at the left-hand side and with a cold reservoir of temperature T_R on the right-hand side. We restrict the width L_y so that it is smaller than twice the diameter $2a$ of the hard disk, i.e., $L_y < 2(2a)$. With this restriction, the particles remain ordered, so a particular particle label corresponds to a particular location in the system. We use a modified microscopic collision rule which models the collision of the hard disks with the interfaces between the system and the reservoirs such that when a particle hits either boundary with velocity (v_x, v_y) it bounces back into the system with the velocity components changed by the reservoir temperature as

$$v_x' = -\,\mathrm{sgn}(v_x)\epsilon_x v_I - (1-\epsilon_x)v_x, \tag{1}$$

$$v_y' = \mathrm{sgn}(v_y)\epsilon_y v_I + (1-\epsilon_y)v_y, \tag{2}$$

where $v_I \equiv \sqrt{k_B T_I/m}$ with T_I being either T_L or T_R. The accommodation coefficient $\epsilon_i (i=x,y)$ varies in between zero and unity: The case of $\epsilon_i=0$ corresponds to the specular boundary condition and that of $\epsilon_i=1$ corresponds to the diffusive boundary condition where a complete reconciliation of the thermal momentum is assumed. In the present work, the transverse velocity is treated not to be changed by the boundary scattering on the interfaces; i.e., we set $\epsilon_y \equiv 0$, and we apply the usual periodic boundary condition in the transverse direction as depicted. This microscopic collision rule was used previously to investigate the instability structure of the phase space [14,15]. The parameters that we use in the simulation throughout are specified here:

$$N = 100, \quad N\frac{(2a)^2}{L_x L_y} \equiv n_0, \quad \epsilon_x = 0.5.$$

In the above n_0 is the density parameter that we introduce and $n_0=0.1$ is chosen for most of data unless otherwise specified.

According to the first law of thermodynamics, the internal energy U of the system changes in the course of simulation as

$$\frac{dU(t)}{dt} = \dot{Q}_L + \dot{Q}_R, \tag{3}$$

where $\dot{Q}_i = dQ_i/dt$ is the rate of the total heat flow into $(i=L)$ and out of $(i=R)$ the system at the corresponding end. Therefore, for a specified temperature ratio T_L/T_R, we anticipate that the system reaches a steady state, when the steady state condition of $\dot{Q}_L = |\dot{Q}_R|$ establishes. By monitoring the energy flow at both ends we are able to decide when the system comes to the desired steady state.

After the system reaches a steady state, we accumulate the discrete velocities of each particle to obtain the velocity histogram. The histogram gives the frequency of finding the velocity in the range $(v_x, v_x+\zeta_x)$ and $(v_y, v_y+\zeta_y)$ at a particular location x, where ζ_l is the velocity bin width in the histogram, $l=x,y$. Here, x is understood to be the average position of the particle of focus. Then, we determine the velocity distribution $g(v_x, v_y; x)$ by normalizing the histogram as

$$\sum_{i,j} g(v_i, v_j; x)\zeta_i \zeta_j = 1, \tag{4}$$

where the indices i,j run over all the velocity bins.

In Fig. 2 we illustrate the reduced velocity distribution of the hard disk, located at the average position x, which is defined as

$$g(v_i; x) \equiv \sum_j g(v_i, v_j; x)\zeta_i \zeta_j.$$

In this work we choose the same bin widths, $\zeta_i = \zeta_j \equiv \zeta_0$, where $\zeta_0 = 0.05$ is in units of the reference velocity v_0 which is defined as $v_0 \equiv \sqrt{k_B T_0/m}$ where T_0 is a reference temperature which is set to be T_R throughout. Note that what are actually drawn in Fig. 2 are the reduced distributions divided by the corresponding local equilibrium ones, accordingly the distributions vanish at large velocities in both directions. The numbers near the curves indicate the label of particle beginning from the left, i.e., hot end of the system. The deviation from local equilibrium appears as an excess of large positive velocities, opposite to the direction of the temperature gradient, which is compensated by a small peak at negative velocities. In addition, we have seen that the y-component ve-

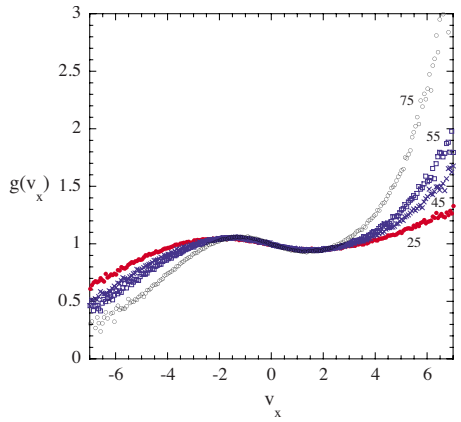

FIG. 2. (Color online) Reduced velocity distributions for QOD hard disks at a temperature ratio of $T_L/T_R=10$, where the numbers denote the labeling of the particles from the hot end. The distributions are normalized by the corresponding local equilibrium distributions and the velocities are in units of v_0, where $v_0 \equiv \sqrt{k_B T_R/m}$.

locity distributions follow essentially the local equilibrium ones, accordingly they are not presented.

In Fig. 3 the typical hydrodynamic profiles are shown as a function of the average positions of the hard disks. Throughout this work positions are to be understood as being in units of the diameter of the hard disks. The local steady-state density is measured in the simulation as

$$n(x) = \frac{1}{\Delta\langle x\rangle L_y}, \tag{5}$$

where $\Delta\langle x\rangle$ is the distance between the half-way points separating the average positions of the particle of interest and that of its nearest neighbor. The i component of the local temperature is measured according to $(i=x,y)$

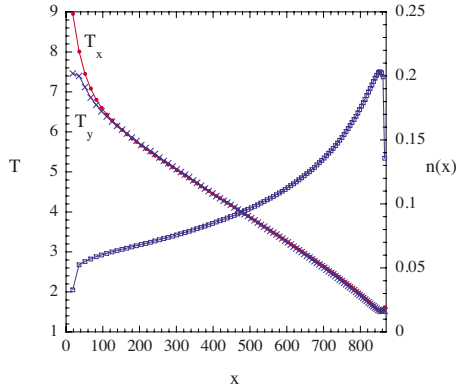

FIG. 3. (Color online) Temperature and density profiles vs average positions for hard disks at $T_L/T_R=10$, where the temperatures are in units of the reference temperature T_R, the density is in units of the inverse of the diameter of the hard disk squared, and the positions are in units of diameter $2a$.

$$\frac{1}{2}k_B T_i(x) = \frac{\sum_l \left[\frac{1}{2}mv_{il}^2\right]\tau_l}{\sum_l \tau_l}, \tag{6}$$

where k_B is the Boltzmann constant and τ_l is the free-flight time of the particle between collisions with constant velocity (v_{xl}, v_{yl}), so $\Sigma_l \tau_l$ is the total measuring time. The temperatures decrease monotonously with the distance from the hot end. On the other hand, the density profile manifests the opposite trend. Near the interfaces with the reservoirs strong boundary effects appear stemming from our microscopic scattering model. Note that $T_x(x)$ is identical with $T_y(x)$ in the bulk, which reflects indirectly that the system reaches the desired steady state, but a discrepancy appears near the boundaries. Although not drawn, the pressure p, from the equilibriumlike relation, $p=nk_BT$, is seen to be relatively constant along the system when the local values of n and T are used. Also, the flow velocity, or the first-order velocity moment, was seen to be vanishingly small in our system as anticipated. Our QOD model produces the steady-state hydrodynamic profiles consistent with the exact solutions to the kinetic equation, reported previously [12,13].

III. GENERALIZED GIBBS RELATION: KINETIC THEORY

Here we describe the kinetic theory basis of NE thermodynamics for our heat transport model so that the discussions of the simulation outcomes that follow are made self-contained. The basic ingredient is the Boltzmann entropy $S(t)$ which is defined, up to a constant, to be

$$S(t) = \int d\mathbf{r} s(\mathbf{r},t), \tag{7}$$

where $s(\mathbf{r},t)$ is the entropy density at position $\mathbf{r}$ at time t given as [16]

$$s(\mathbf{r},t) = -k_B \int d\mathbf{v} f(\mathbf{r},\mathbf{v},t) \ln f(\mathbf{r},\mathbf{v},t). \tag{8}$$

The distribution function $f(\mathbf{r},\mathbf{v},t)$ obeys the Boltzmann equation which takes the following form without external forces,

$$\frac{\partial f}{\partial t} + \mathbf{v}\cdot\frac{\partial f}{\partial \mathbf{r}} = J[f], \tag{9}$$

where $J[f]$ is the collision integral. The distribution function is normalized as

$$\int d\mathbf{v} f(\mathbf{r},\mathbf{v},t) = n(\mathbf{r},t), \tag{10}$$

where n is the local number density of the system.

In kinetic theory the local entropy-balance equation is derived theoretically by calculating the total time derivative of the Boltzmann entropy, Eq. (7), with use of the Boltzmann equation, Eq. (9). The result is expressed as

$$\frac{\partial s}{\partial t} + \nabla \cdot \mathbf{j}_s = \sigma_{ent}. \tag{11}$$

In the above the entropy flux $\mathbf{j}_s$ is given by

$$\mathbf{j}_s(\mathbf{r},t) = -k_B \int d\mathbf{v}\mathbf{v} f \ln f. \tag{12}$$

Also, the entropy-production per unit volume σ_{ent} is given by

$$\sigma_{ent}(\mathbf{r},t) = -k_B \int d\mathbf{v} J[f] \ln f, \tag{13}$$

which is positive according to H theorem [3]. Accordingly, all the local quantities associated with the entropy balance equation have been defined through the solution to the Boltzmann equation rigorously. It is important to note that their definitions are exact within the validity of the Boltzmann equation, and are not restricted to the linear regime. In our MD formulas these exact definitions are used.

Hereafter, we specialize our discussion to the QOD system with a temperature gradient along negative x. The flow velocity does not enter into the current problem because the total momentum must be conserved on average. Also, time dependence is removed for a steady-state system. Further, we consider a small temperature gradient in order to provide a concrete theoretical description of the well-adapted linear irreversible thermodynamics for our system. When one seeks for the Chapman-Enskog expansion solution to first order in the gradient, i.e., Navier-Stokes order [17], the distribution function is given as

$$f = f_L + \Phi. \tag{14}$$

In the above f_L is the local-equilibrium distribution function which reads

$$f_L(x,\mathbf{v}) = \exp\left[\left\{\mu(x) - \frac{1}{2}mv^2\right\}\beta(x)\right], \tag{15}$$

where μ is fixed by the normalization condition, Eq. (10), as

$$\mu(x) = \beta(x)^{-1} \ln\left\{n(x)\left(\frac{m\beta(x)}{2\pi}\right)^{d/2}\right\},$$

where d is the dimensionality and $\beta = 1/(k_B T)$. The deviation from the local equilibrium is obtained at the first Sonine approximation explicitly as [7]

$$\Phi(x,\mathbf{v}) = -\nu^{-1} f_L\left(\frac{1}{2}m\beta v^2 - \frac{d+2}{2}\right) v_x \frac{d\ln T}{dx}, \tag{16}$$

where the coefficient ν^{-1} is by

$$\nu^{-1} = \frac{2}{d+2}\frac{m}{k_B}\kappa p^{-1}, \tag{17}$$

in which p and κ are the hydrostatic pressure and the thermal conductivity, respectively.

It is worthwhile to note that the spatial dependence of solution, Eq. (14), occurs only through the hydrodynamic fields, which is a well known characteristic of a *normal* solution to the Boltzmann equation [13]. Accordingly, it follows that any velocity moments will possess similar dependence. For instance, the heat flux of the structure, whose definition is given by $\mathbf{j}_Q = \int d\mathbf{v} \frac{1}{2} m v^2 \mathbf{v} f$, can be calculated explicitly using the distribution function given in Eq. (14) to obtain

$$\mathbf{j}_Q(x) = -\kappa \frac{dT}{dx}\hat{x}, \tag{18}$$

which is nothing but Fourier's law. In addition, since the local energy balance implies in the steady state that

$$\nabla \cdot \mathbf{j}_Q(x) = 0, \tag{19}$$

the heat flux must be uniform in the present problem. This is in contrast to the entropy balance in nonequilibrium states in which the entropy flux is nonuniform according to

$$\nabla \cdot \mathbf{j}_s = \sigma_{ent}. \tag{20}$$

Next, one can substitute the Chapman-Enskog expansion solution into Eqs. (8), (12), and (13) and carry out the velocity integration. The results are given below to leading order in the temperature gradient in each case: The entropy density is obtained at the level of the local-equilibrium approximation,

$$\begin{aligned} s(x) &\simeq -k_B \int d\mathbf{v} f_L \ln f_L \\ &= k_B n(x)\left[\frac{d}{2} - \ln\left\{n(x)\left(\frac{m\beta(x)}{2\pi}\right)^{d/2}\right\}\right], \end{aligned} \tag{21}$$

which is reminiscent of the equilibrium Sackur-Tetrode equation except that the hydrodynamic fields are local in the present case. The entropy flux is given to Navier-Stokes order as

$$\mathbf{j}_s(x) \simeq -k_B \int d\mathbf{v}\mathbf{v}\Phi \ln f_L = -\kappa T^{-1}\frac{dT}{dx}\hat{x}. \tag{22}$$

Utilizing Eq. (18), one can cast the expression for the entropy flux into the form

$$\mathbf{j}_s(x) = T^{-1}\mathbf{j}_Q(x) \tag{23}$$

whose physical significance is discussed below. For the entropy production, instead of using Eq. (13), one may calculate it from Eq. (20) under the steady-state condition as

$$\sigma_{ent}(x) = \nabla \cdot (T^{-1}\mathbf{j}_Q) \simeq \kappa \left|\frac{d\ln T}{dx}\right|^2, \tag{24}$$

where in the second step use has been made of Eq. (19). The positivity of the local entropy-production rate manifests itself in Eq. (24). Note that all the spatial dependence of the entropy density, flux, and production rate are implicit through the local temperature, which reflects the aforementioned aspect of the normal solution to the kinetic equation.

The relation, Eq. (23), between the entropy flux and the heat flux may be viewed as the generalized version of the equilibrium Clausius relation. It constitutes an underlying basis of the linear irreversible thermodynamics for steady-state heat transport in our system. When Eq. (23) is combined with the first law of thermodynamics, one establishes the generalized Gibbs relation in the form,

$$T_{st}ds = de - \left(\frac{p_{st}}{n} + \mu_{st}\right)dn, \tag{25}$$

where T_{st}, p_{st}, and μ_{st} are the local, steady state, temperature, pressure, and chemical potential, respectively. Note that Eq. (25) views the entropy density as $s=s(e,n)$ where the NE conjugate to the number density n is characterized formally as a combination of the pressure and the chemical potential. The energy density $e(x)$ is specified by the definition, $e(x)=\int d\mathbf{v}\frac{1}{2}mv^2 f(x,\mathbf{v})$ which gives $e=\frac{d}{2}nk_BT$. Then, the steady-state temperature T_{st} is determined from the partial differentiation,

$$T_{st}^{-1} = \left(\frac{\partial s}{\partial e}\right)_n, \tag{26}$$

and with use of Eq. (21) it turns out that

$$T_{st}(x) = T(x). \tag{27}$$

Similarly, the steady-state pressure is calculated from

$$p_{st} = -n\left\{\mu_{st} + T_{st}\left(\frac{\partial s}{\partial n}\right)_e\right\}, \tag{28}$$

which, utilizing $\mu_{st}=\mu$, results in

$$p_{st}(x) = p(x). \tag{29}$$

In obtaining Eq. (29) we have defined the kinetic pressure p as one-half of the trace of the pressure tensor for the present QOD model ($d=2$), accordingly $p=nk_BT$, as was used in the previous section to calculate the hydrodynamic pressure profiles. Then, it follows that $p_{st}=nk_BT_{th}\to p$. Thus, the steady-state temperature and pressure are identical locally to the kinetic temperature and pressure in the linear heat transport problem.

IV. LOCAL ENTROPIES: SIMULATION RESULT

For the low-density system considered the quantities associated with the entropy balance are defined explicitly in terms of the distribution function via the Boltzmann entropy. We adopt the theoretical definitions for the entropy density, flux, and entropy production, as given in Eqs. (8), (12), and (13), and evaluate them numerically utilizing the velocity distribution data measured from our NEMD. To this end, we first need to make the equations discrete in the velocity scale of ζ_0 which is the bin size of our MD velocity measurement. In the following it is to be understood that all distances are normalized by $2a$ and the velocities by v_0 which is defined in Sec. II.

Before proceeding, it is worthwhile to note that the factor of $\ln f$ appearing in the conventional definition of the Boltzmann entropy, Eq. (7), is not well defined in the sense that the argument f has the dimensions of $1/(2av_0)^d \equiv \alpha^{-1}$. This logarithmic factor enters subsequently in each of Eqs. (8), (12), and (13). Accordingly, it must be made dimensionless, in particular, for our numerical purposes. That can be done by a transformation $f\to\bar{f}=f\alpha$ which leads to $\ln f\to\ln\bar{f}-\ln\alpha$ in the relevant equations. Of course, α still has the dimensions of the inverse of f; however, when all the extra terms, generated by $\ln\alpha$ in Eqs. (8), (12), and (13), are gathered, together they give

$$k_B\left\{\frac{\partial n}{\partial t} + \nabla\cdot(n\mathbf{u})\right\}\ln\alpha,$$

in the entropy balance equation, Eq. (11), where $\mathbf{u}$ is the flow velocity. Therefore, when there are no sinks or sources of particles in the system, the additional term gives no contribution. Accordingly, the factor $\ln f$ does not cause any problem even though the argument f has dimensions.

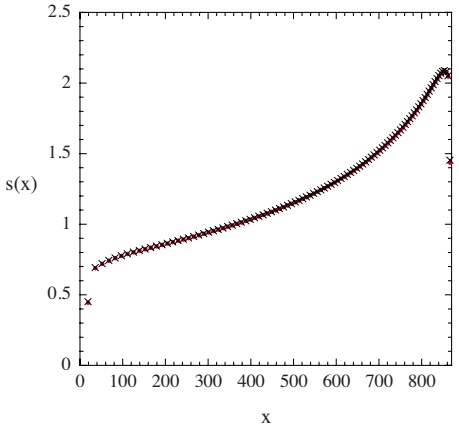

FIG. 4. (Color online) Entropy density along the system for a fixed temperature ratio of $T_L/T_R=10$, where the entropy density is in units of $k_B/(2a)^2$.

In Fig. 4 we draw a representative entropy density of the QOD system for a fixed temperature ratio. The bullets are the outcome of the numerical simulation, calculated from the coarse-grained formula of Eq. (8),

$$[s(x)]_{\mathrm{MD}} = -n^*(x)\sum_{i,j}\bar{g}(v_i,v_j;x)\ln\bar{g}(v_i,v_j;x) - n^*(x)\ln n^*(x), \tag{30}$$

where the dimensionless distribution function $\bar{g}$ is defined in terms of the measured distribution function g from NEMD as

$$\bar{g} \equiv g(2a)^2\zeta_0^2/n^*.$$

Also, the entropy density is made dimensionless according to $[s]_{\mathrm{MD}}\equiv s(2a)^2/k_B$ and the density as $n^*\equiv(2a)^2n$. The crosses are the results from the Sackur-Tetrode equation, Eq. (21), after substitution of the simulated hydrodynamic profiles. As one can see, the two results match quite well throughout the system. There appears an abrupt change in the entropy density close to the interfaces where significant boundary effects occur. There is more entropy locally at a position with a colder temperature compared to a higher temperature region where the particle density is lower.

In Fig. 5 the entropy flux is given for the same system and temperature ratio used in Fig. 4. The entropy flux has been obtained from the discrete formula in Eq. (12),

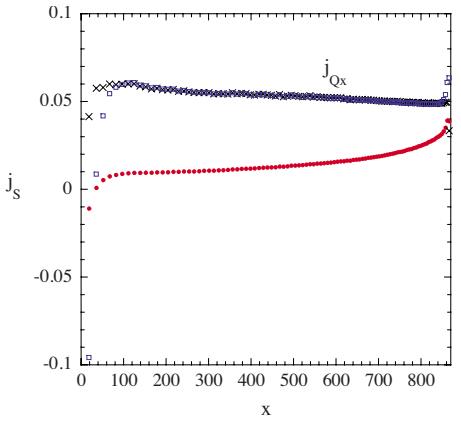

FIG. 5. (Color online) Entropy flux along the system for a fixed temperature ratio of $T_L/T_R=10$, where the entropy flux is represented by the bullets and is in units of $k_B v_0/(2a)^2$.

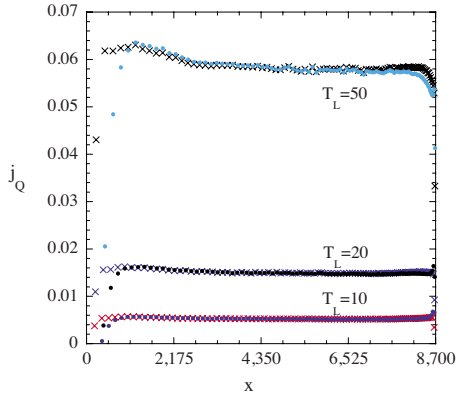

FIG. 6. (Color online) Heat flux along the system for several temperature ratios, $T_L/T_R=10$, 20, and 50 at a density parameter of $n_0=0.01$, where the heat fluxes are in units of $k_B T_0 v_0/(2a)^2$ and T_L is normalized by T_R.

$$[j_s(x)]_{\mathrm{MD}} = -n^*(x)\sum_{i,j} v_i \bar{g}(v_i,v_j;x)\ln \bar{g}(v_i,v_j;x), \quad (31)$$

which is made dimensionless by dividing it by $k_B v_0/(2a)^2$. The result shows that the steady-state entropy flux increases toward the cold end, which can be understood from Eq. (19). Since the heat flux is uniform, it follows that $j_s(L)/j_s(R)=T_R/T_L$. Accordingly, for $T_L>T_R$ it implies that $j_s(L)<j_s(R)$. We have also calculated the entropy flux from the simulated heat flux by dividing it by the local temperature. The heat flux was obtained from the discrete version of its kinetic theory definition,

$$[j_Q(x)]_{\mathrm{MD}} = n^*(x)\sum_{i,j}\left[\frac{1}{2}(v_i^2+v_j^2)v_i\right]\bar{g}(v_i,v_j;x), \quad (32)$$

which is made dimensionless by dividing both sides with $k_B T_0 v_0/(2a)^2$. We found that the entropy fluxes obtained by the two methods are identical within numerical accuracy throughout the structure except near the walls. To illustrate these findings, we plot the heat flux in the same Fig. 5 together with the entropy flux under the same conditions. In the figure the crosses are obtained directly from the heat flux which is nearly constant throughout the structure as expected. The apparent slope of the heat flux is due to the neglect of collisional contributions which vary with density (and hence position). The entropy flux multiplied by the local temperature is presented as the unfilled squares, which agrees well the heat flux in the bulk. The difference shown near the walls is again attributed to the strong boundary effects in our QOD collision model. Consequently, we confirm that the generalized Clausius relation Eq. (23) for the steady state holds quite well, which in turn asserts that the kinetic temperature is equal to the NE, steady-state temperature locally in the QOD heat transport system.

In order to examine the generalized Clausius relation further in the regime where kinetic theory is accurate, we have carried out the same calculation for several temperature ratios, $T_L/T_R=10$, 20, and 50 for a lower density of $n_0=0.01$. The results are depicted in Fig. 6 where the bullets are the data from the entropy flux multiplied by the temperature profile for each temperature ratio. There appear well-defined bulk heat fluxes for the temperature ratios, $T_L/T_R=10$ and 20, and in these cases the generalized Clausius relation, represented by the bullets, works well except near the boundaries. However, it is seen that at the temperature ratio of $T_L/T_R=50$ the two heat-flux profiles match with each other not as good as the smaller temperature ratios. Accordingly, it seems that the temperature ratio of $T_L/T_R=50$ is too large for the generalized Clausius relation to hold accurately. Therefore, it suggests that linear irreversible thermodynamics fail to work away from the small-gradient regime as predicted by the kinetic theory. There appears a marginal variation in the bulk heat-flux in Fig. 6 for $T_L/T_R=50$ which seems not to satisfy the strict spatial constancy of the heat flux, Eq. (19). As noted previously in Fig. 5, this is due to the neglect of the collisional contributions. Using the exact expression for the bulk heat-flux [1] we have confirmed that it is identical at both ends of the system and that this agrees with the result for the whole system. Within the scope of the Boltzmann entropy we report only the kinetic part.

Next, we consider the entropy-production rate in Fig. 7 which is calculated using the MD formula,

$$[\sigma_{ent}(x)]_{\mathrm{MD}} = [n^*(x)]^2[T^*(x)]^{1/2}\sum_{i,j}[\bar{g}(v_i,v_j;x) - \bar{g}_L(v_i,v_j;x)]\ln[\bar{g}(v_i,v_j;x)/\bar{g}_L(v_i,v_j;x)], \quad (33)$$

which was made dimensionless by dividing it with $\nu_0 k_B\sqrt{T_0}$, where $\bar{g}_L$ is the dimensionless local-equilibrium distribution function given by

$$\bar{g}_L(v_i,v_j;x) \equiv \frac{\zeta^{*2}}{2\pi T^*(x)}\exp\left[-\frac{1}{2}(v_i^2+v_j^2)/T^*(x)\right],$$

in that the temperature profile is normalized as $T^*=T/T_0$ where $T_0=T_R$ and also that $\zeta^*\equiv\zeta/v_0$. Equation (33) is a discrete version of Eq. (13) where for computational simplicity the collision integral is replaced by the Bhatnagar-Gross-Kook (BGK) kinetic model [18],

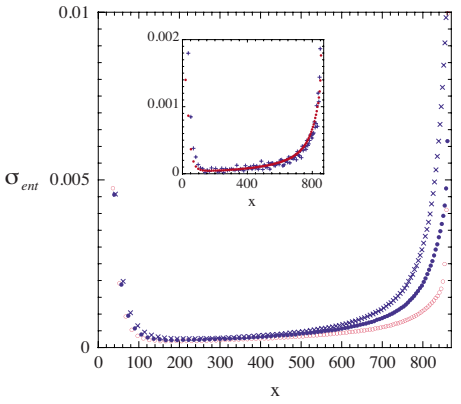

FIG. 7. (Color online) Entropy production rate along the system for the chosen temperature ratios of $T_L/T_R=10$ (circles), 20 (bullets), and 50 (crosses), where the entropy production rates are in units of $\nu_0 k_B \sqrt{T_0}$. The inset is the comparison between two results for $T_L/T_R=10$, where the plus symbols are from Eq. (20) and the bullets are from Eq. (33).

$$J[f] \to -\nu(x)(f - f_L),$$

where ν is the average collision frequency whose relation to the thermal conductivity is given in Eq. (17). When it is evaluated with the local equilibrium distribution function, it turns out that

$$\nu(x) = \nu_0 n(x)\sqrt{T(x)},$$

for both hard disks ($d=2$) and spheres ($d=3$), where ν_0 is a constant, independent of x, whose specific value depends on the dimensionality. It is well known that the BGK model preserves the most important features of the Boltzmann equation. Collaterally, the entropy-production rates can be calculated using Eq. (20) by taking derivative of the already obtained entropy fluxes numerically. Both approaches are not limited to the small gradient regime. We have confirmed that the results from Eq. (20) and (33) are identical, up to an overall constant which arises from the different normalization schemes, within the numerical accuracy (see the inset). The results shown in Fig. 7 are for several temperature ratios, where the empty circles are for $T_L/T_R=10$, the filled bullets are for $T_L/T_R=20$, and the crosses are for $T_L/T_R=50$. We see that the entropy-production rates are positive at all points in the system. The bigger temperature ratio, the bigger the entropy-production rate. Also, the boundary effects are shown near the walls. The slow increase of the entropy-production rate in the bulk toward the cold end may be understood from Eq. (24), which states that $\sigma_{ent} \sim T^{-3/2}$, assuming constant temperature gradients. When the temperature gradient is small, the entropy production rate obeys the phenomenological expression of linear irreversible thermodynamics, given in Eq. (24).

Finally, we present the total entropy of the system for various temperature ratios. The total steady-state entropy for a fixed temperature ratio between the two ends is calculated from

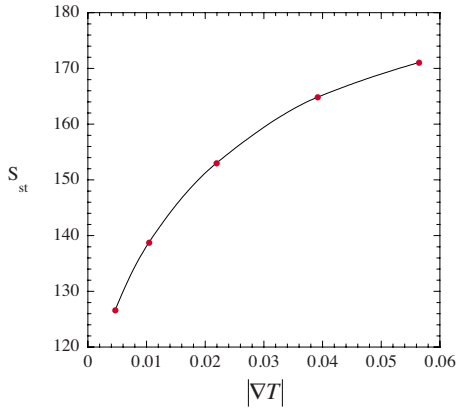

FIG. 8. (Color online) Total entropy vs temperature gradient $|\nabla T|$ for $T_L/T_R=5$, 10, 20, 35, and 50; the entropy and temperature gradient are in units of $k_B L_y/(2a)$ and $T_0/(2a)$, respectively.

$$S_{st} = L_y \int dx s(x). \tag{34}$$

The numerical result is given in Fig. 8 where the steady-state entropy is drawn as a function of the temperature gradient which is defined to be

$$|\nabla T| \equiv \frac{T_L - T_R}{L_x}.$$

For the present purpose we used $L_y=1.15\times(2a)$ and the corresponding L_x was determined by $L_x=n_0\times L_y/[N(2a)^2]$ with $n_0=0.1$. It is seen that the steady-state entropy of the system increases monotonically with the temperature ratio. Linear irreversible thermodynamics is applicable only to the small temperature ratio domain. In the opposite regime the generalized Gibbs relation does not hold, however the applicability of the Boltzmann entropy extends to such a far from equilibrium limit.

V. CONCLUSION

We have considered a QOD system of hard disks, placed in thermal contact at each end with a heat reservoir at a different temperature to generate heat transport. The system is closed diffusively, however, it is subject to a thermodynamic force which produces the temperature gradient. We have performed MD simulations to study the local properties of irreversible thermodynamics employing the Boltzmann entropy as the NE entropy. Consequently, we have obtained the *inhomogeneous* entropy densities, fluxes, and production rates along the system, associated with the entropy balance in the steady state.

Our simulation is not limited to the situation of a small temperature gradient, however, our attention has been largely directed to the linear regime where the phenomenological description of irreversible thermodynamics provides a comparison. In the linear regime it is shown that the entropy flux at a chosen position, multiplied by the local kinetic temperature at the corresponding point, equals the local heat flux. This means that the equilibrium-like Clausius relation holds

locally in our system, which, in turn, asserts that the kinetic temperature is identical with the NE thermodynamic temperature in the steady state. A proper definition of temperature for NE states is a continually important issue [19]. We have manifested it in a concrete example of a QOD heat flow by computer experiments. We have combined the local Clausius equation with the first law of thermodynamics to constitute the generalized Gibbs relation of linear irreversible thermodynamics in local form. In the case when the temperature gradient departs from the linear response regime, the numerical data suggest that the generalized Gibbs equation no longer hold. Our simulation outcome is consistent with the kinetic theory prediction.

In short, we have investigated the NE thermodynamics of the heat transport problem using MD simulations in the steady state. The *nonuniform* Boltzmann entropy density served as the relevant NE thermodynamic potential for the low-density system considered. We have verified the direct local information on the entropy balance of the QOD system by computer experiments. The simulations of the QOD system are not limited in any way, so this system provides a very useful test bed to determine the accuracy or otherwise of theories which extend the Boltzmann entropy beyond the low-density or linear regimes.

ACKNOWLEDGMENTS

C.S.K. acknowledges the support from the Chonnam National University, 2008, to spend a sabbatical and also the partial support from the Gordon Godfrey Fund at the School of Physics in the University of New South Wales.

[1] See, for instance, D. J. Evans and G. P. Morriss, *Statistical Mechanics of Nonequilibrium Liquids* (Cambridge University, Cambridge, 2008).
[2] S. R. de Groot and P. Mazur, *Nonequilibrium Thermodynamcis* (Dover, New York, 1984).
[3] C. Cercignani, *The Boltzmann Equaitons and Its Applications* (Spinger-Verlag, New York, 1988).
[4] See, for instance, T. Taniguchi and G. P. Morriss, Phys. Rev. E **70**, 056124 (2004) and references therein.
[5] J. J. Brey and A. Santos, Phys. Rev. A **45**, 8566 (1992).
[6] J. M. Montanero and A. Santos, Physica A **225**, 7 (1996).
[7] V. Garzó and A. Santos, *Kinetic Theory of Gases in Shear Flows* (Kluwer Academic, Dordrecht, 2003).
[8] P. Resibois, J. Stat. Phys. **19**, 593 (1978).
[9] M. Mareschal, Phys. Rev. A **29**, 926 (1984).
[10] D. J. Evans, J. Stat. Phys. **57**, 745 (1989).
[11] A. Baranyai and D. J. Evans, Mol. Phys. **74**, 353 (1991).
[12] A. Santos, J. J. Brey, C. S. Kim, and J. W. Dufty, Phys. Rev. A **39**, 320 (1989).
[13] C. S. Kim, J. W. Dufty, A. Santos, and J. J. Brey, Phys. Rev. A **39**, 328 (1989).
[14] T. Taniguchi and G. P. Morriss, Phys. Rev. E **68**, 026218 (2003).
[15] T. Taniguchi and G. P. Morriss, C. R. Phys. **8**, 625 (2007).
[16] In literature one cast the entropy density often into $s \rightarrow -k_B \int d\mathbf{v} f(\ln f - 1)$. The manipulated term adds simply a constant to the total entropy for a diffusively closed system, which, of course, does not affect the change of total entropy. However, the additive constant, which becomes null under time derivative, is ambiguous within a miltiplicative factor; thus the entropy density, which is local, is not uniquely defined if we admit such a procedure in our case.
[17] J. R. Dorfman and H. van Beijeren, in *Statistical Mechanics, Part B: Time-Dependent Processes*, edited by B. Berne (Plenum, New York, 1977).
[18] R. Zwanzig, *Nonequilibrium Statistical Mechanics* (Oxford University Press, New York, 2001).
[19] See, for instance, a latest report by Wm. G. Hoover and C. G. Hoover, Phys. Rev. E **77**, 041104 (2008).